

Response to the Review

of

Leon Thomsen, 03 Nov 2024

Line 46. This statement is probably not true, and in any case should be supported with references. A better statement would be, "A commonly studied type of seismic anisotropy..."

- We see your point that this statement is too strong and lacks appropriate references. We will change it accordingly in the revised manuscript.

Line 55. It should be specified here that C_{ij} is measured in the principal coordinate system of the medium, not the survey coordinate system.

- We fully agree, that this is not specifically mentioned in the manuscript. We will add this information to make it clear, that these two coordinate systems differ from each other.

Line 57. These phase velocities are correct, but the data measure group (ray) arrival times, hence group (ray) velocities, at ray angles, not phase angles. The authors should discuss these issues, referring e.g. to Thomsen (1986).

- You raise an important point regarding the distinction between group (ray) velocities and phase velocities. While we recognize that the two differ, the weak anisotropy in our case suggests that the differences are not significant. Additionally, our analysis includes other simplifications, such as a homogeneous medium, which are likely to have a greater impact on the results.

Line 70. The reference here should not be "near-vertical", but rather "close to the symmetry axis", which differs from the vertical in TTI media.

- Thank you for this important aspect, you are right that this is not the same in the present medium and will be corrected accordingly.

Line 102. It appears from Fig. 1 that the boreholes all lie in or close to the vertical plane beneath the tunnel. It would be useful to rotate the inset in Fig. 1 to align with that plane, thus showing the deviations (if any) from the plane. If the data are all co-planar, that reduces their ability to describe tilted orthorhombic symmetry.

- We appreciate your remark that the orientation of the boreholes may not be clear enough to the reader. One big advantage of the study presented in this work is precisely this aspect, that the orientation of the tripod boreholes allows measurements of direct seismic waves in 3D, unlike many other crosshole seismic surveys covering mostly only 2D planes. To point this out, we will add the information of the tunnel orientation in Tab. 1 as a reference direction and provide more plots and additional material, showing the orientation of the boreholes. This should then make the used source-receiver positions clearer.

Line 124. This claim needs a reference.

- You are right that we should verify this statement further. The sparker used here is a monopole source in a water-filled borehole. The energy discharge generates a pressure pulse in the water which initially spreads isotropically and therefore also excites the borehole wall isotropically (Singer 2007, Ch. 18.5). We will change this paragraph accordingly in the manuscript.

Line 127. This “explanation” is misleading. A better explanation would be, “This can be explained by P-S conversion at the borehole wall near to the source..”

- We agree with this comment and modify this section accordingly.

LINE 134. This 3C orientation issue results in a MAJOR limitation in the analysis. The geophones may be oriented from the data itself, assuming vector fidelity (c.f. Gaiser, 2007, Geophysics, 72(3), p. V67–V77). For each geophone-source pair: a) Rotate (3D) the 3C data such that the energy in the P-wave window is maximized on the new x3 axis, which is now aligned with the incoming P-wave polarization, which is close to the P-wave propagation vector. (If this is not pointing back at the source, then either the medium is not uniform (as assumed), or the data are not vector-faithful (as assumed).) b) Rotate about the new x3 axis such that the cross-correlation of the x1 and x2 traces is maximized, with a cross-correlation lag. The geophone is now aligned (3D) in the principal coordinate system, with the three modes separated onto the three axes. c) If you assume (as you apparently do below), that S1 is the SH mode, then this specifies the new x1 axis as lying in the TTI plane of symmetry, which by assumption is the same for all geophones, and is determined absolutely from the P-wave velocities as you describe. d) These rotations, run backwards, determine the original orientation of the geophone. e) The same operation, with the same geophone but different source, should yield the same geophone orientation and the same orientation of the principal coordinate system; if not you can minimize the misfit, or use the differences to refine the assumptions. f) With the 3C data now fully specified, your analysis is more robust, including analysis of shear-wave polarizations.

- We highly appreciate your input on the analysis of the 3C geophone data. The proposed approach could indeed help to use the measured data for an advanced analysis, especially of the S-wave arrivals. Unfortunately, we have to conclude that the available data quality does not allow such an analysis. Even the first step, aligning the x3 component with the incoming energy, is not reliably possible. There are various reasons that prevent this analysis:
 - The quality of the 3C geophone data is in general very weak. About 25% of the measurement points cannot be used because at least one channel per measurement point is either too noisy or dead.
 - The original orientation of the components perpendicular to the borehole (x1, x2) are not known so that the rotation angle around the x3-component along the borehole cannot be interpreted.
 - In a considerable amount of source-receiver pairs a tube- or reflection wave is recorded in addition to the direct waves. These waves are polarized differently than the P- and S-waves and therefore appears even after the rotation on several components and overlays the signal of interest.
 - After the first rotation step (maximizing the P-wave energy on one component), most of the sensors show a maximized energy direction in the horizontal plane, independent of the source or receiver position. However, we do not assume that this describes the actual incoming wave direction, as no pattern with the measurement geometry can be found. We rather assume that this is due to the poor coupling of the sensor with the rock. This reduces the directional dependency of the sensors.

The sensors used in this study were the only available and reasonably usable sensors under the given conditions. The sensors were “clamped” on the borehole wall by an inflatable bike tube, strongly influencing the data quality. We assume that this clamping mechanism is damping incoming waves from one side and also reduces the sensitivity of the vertical component, along the borehole.

Even though that the proposed analysis did not work, the 3C geophone data are still helpful to identify the recorded signals as S-waves. Fig. A1 of the manuscript shows that the different wave types (here, P- and S1 wave) appear even in the unrotated case on different components, proving the different polarization directions of the waves. This knowledge proves the appearance of the different wave types in the measurements.

LINE 203, Table 3. This table shows the result that $\epsilon < \delta$, which results in unusual SV-wave propagation (cf. Tsvankin and Thomsen, 1994, Geophysics, 59(8), 1290-1340). If this result survives the more robust 3C analysis described above, the authors should comment.

- We understand your concern regarding the magnitude of the different parameter describing the anisotropy in the final model. However, many studies investigating anisotropy are related to sedimentary rocks, which is only partially comparable. While many of these studies indeed show a reversed ratio of ϵ and δ , there are also examples with the same trend as in our study with $\epsilon < \delta$. For example, in Thomsen (1986) Tab. 1, about 1/3 of the examples show $\epsilon < \delta$ and Horne (2013) states that about 25% of mudrocks have a negative ellipticity ($\epsilon < \delta$). Also, some studies in igneous rocks conclude that $\epsilon < \delta$ is a realistic scenario (e.g. Doetsch (2020), Boese (2022)). These studies are also assumed to be more representative for our study, as the analyzed rock type is closer to the Rotondo Granite in Bedretto. We will add this discussion of the parameter in the revised manuscript to set our result in a broader context.

Line 226. Here the authors assume that $S1=SH$. This should be discussed.

- Thank you for this comment, we are pleased to add a detailed discussion of this assumption in the revised manuscript. In general, the SV and SH wave have the same velocity β_0 along the symmetry axis. With increasing angle from the symmetry axis, the SH wave velocity increases, reaching its maximum at 90° in the symmetry plane. In contrast to that, the SV wave velocity increases or decreases up to an angle of 45° and then goes back to its velocity β_0 in the symmetry plane. Thus, the velocity pattern with increasing angle to the symmetry axis is different for the different wave types. Furthermore, the SV wave cannot be the faster wave in the symmetry plane for $\gamma > 0$, which is usually the case (e.g. Thomsen (1986), Horne (2013)). Fig. 1 shows the velocity distribution of the apparent velocities for the different wave types w.r.t. the angle with the symmetry axis. In Fig. 1b, the yellow data points show a dominant trend of increasing velocities with increasing angle to the symmetry axis. As explained above, this pattern can not be explained by SV waves, being symmetric around 45° . This shows that the faster S-wave recorded in the different surveys corresponds to the SH-wave, polarized perpendicular to the symmetry axis. Fig. 1 will be added to the revised manuscript to add this information also to the paper.

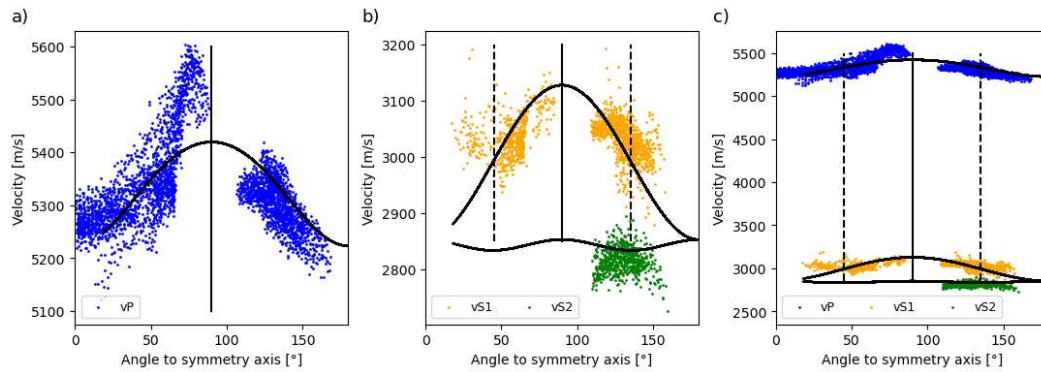


Figure 1. Apparent velocity distribution with increasing angle to the symmetry axis. (a) P-wave velocity, (b) S1 and S2 waves (c) all wave types. Each color corresponds to one wave type (blue = P-wave, yellow = S1-wave and green = S2-wave).

Line 265. This is a strange result. Authors should show how the measured VS2 compare with VSV for their preferred model, as a function of angle.

- We appreciate the observation that the S2 wave velocity shows only small variations and the idea of showing it in comparison with the computed SV velocity. The comparison of the optimized model for VSV with the measured data VS2 is also shown in Fig. 1 (green dots). This plot shows again, that the S2 wave can only be picked in very limited propagation directions. Thus, we can not rule out that the minimum or maximum velocity is missed, which could potentially increase the velocity variation in the medium. However, these data indeed don't show a strong variation of the velocity with the angle to the symmetry axis. The slight variation that is recognizable in Fig. 1b can also be explained by the picking uncertainty for this wave type and relates more to a general dispersion of the variation than a clear trend.

Based on the optimized model, which is also controlled by the other two wave types (ϵ & δ are also controlled by the P-wave), also no strong variation of the velocity is expected for the slower SV wave.

Line 324. The logging data undersample near-vertical fractures.

- You are right that near-vertical fractures are undersampled in the case of vertical boreholes. More generally, fractures that are aligned with the borehole axis tend to be undersampled. In Terzaghi (1965), the relation between the angle between fractures and the borehole and the number of joints, crossing the borehole is analyzed. Based on this analysis, Palmström et al. (1996) state, that fractures with an angle up to 16° have the lowest probability to cross the borehole. In Fig. 2, the poles of fractures (sub-)parallel to the different boreholes as well as to the tunnel are plotted in a stereonet representation (solid line). The dashed lines show the range of fractures with angles of $\pm 16^\circ$ to the borehole. This figure shows, that the combined interpretation of all three boreholes with different orientations and the tunnel does not undersample any fracture orientation.

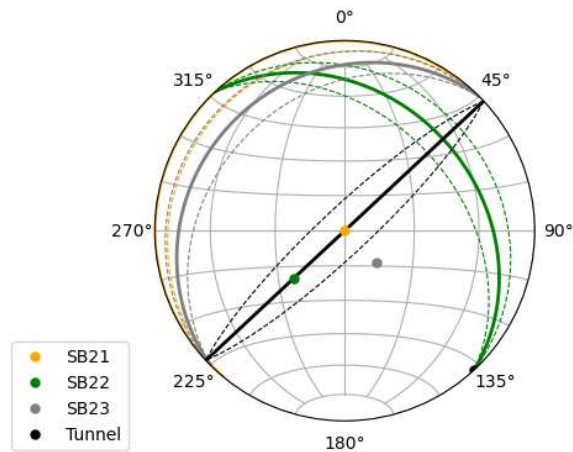


Figure 2. Orientation of the normals of fractures (near-) vertically to the borehole and the tunnel. Solid lines show the orientation of fracture normals for fractures parallel the borehole. Dashed lines show the orientation of fracture normals for fractures with +/- 16° to the borehole orientation. Single dots show the orientation of the corresponding boreholes and the tunnel itself.

Line 228-331. These borehole methods estimate the stress in the immediate vicinity of the borehole, whereas the overburden load varies along the ray paths. Authors should discuss the issue of stress heterogeneity.

- You raise an important point here. Indeed, the vertical stress varies with increasing depth due to the overburden load, while the horizontal stress does not directly correlate with depth but rather appears to be influenced by other factors (e.g., proximity to fractures) (Bröker and Ma (2022)). For an overburden of about 1km and a vertical expansion of the rock volume of interest of 30m, the vertical stress varies of about 3%. In Fig. 3, we compare the variation due to this stress heterogeneity with the variation due to the propagation direction of the signal. The data show a velocity increase with depth of not more than 100 m/s for comparable propagation directions, while the velocity increase due to the increasing angle to the symmetry axis is in the range of 400 m/s for comparable depth steps for P-waves. Thus, the velocity difference due to the stress-increase with depth is small compared to the velocity difference due to anisotropy. In addition, the values mentioned above only represent the extremes for depth differences of +/- 30m. For most signals, the difference between source and receiver depth is less than 30m, so that the effect of the stress heterogeneity on the velocity is even smaller than 100 m/s.

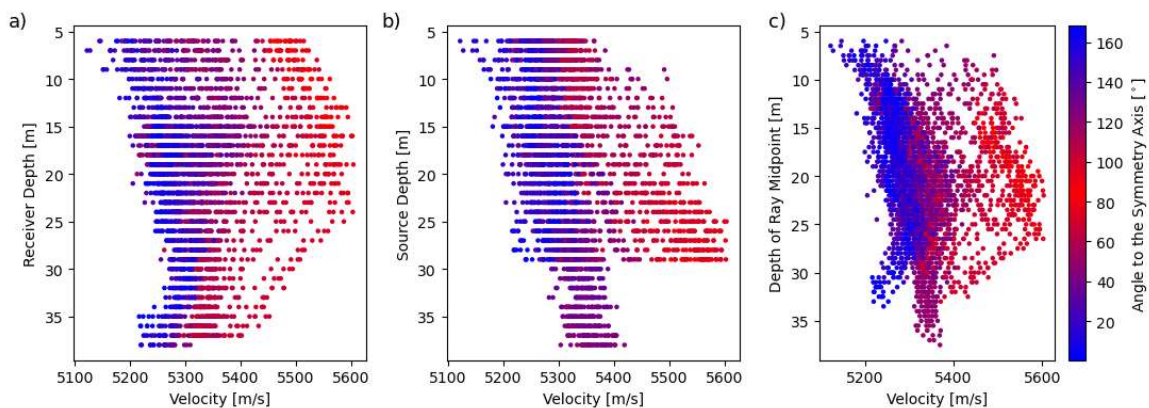


Figure 3. Velocity variations with increasing depth and angle to the symmetry axis. The y axis shows the depth of receiver (a), source (b) and midpoint (c), respectively. The colorbar shows the angle between the symmetry axis and the straight ray.

Line 456. Authors: provide the name of the university for this Ph. D. thesis.

- Thank you for this comment. The thesis is submitted to the research collection of ETH Zurich and will be available soon. The DOI will of course be added to the reference list of the manuscript. Unfortunately, there is a mistake in the reference list of the manuscript, it's not a PhD thesis but a master thesis. We will correct this and I'm very sorry for this mistake.

References:

Boese, C. M., Kwiatek, G., Fischer, T., Plenkers, K., Starke, J., Blümle, F., Janssen, C., & Dresen, G. (2022). Seismic monitoring of the STIMTEC hydraulic stimulation experiment in anisotropic metamorphic gneiss. *Solid Earth*, 13(2), 323–346. <https://doi.org/10.5194/se-13-323-2022>

Bröker, K., Ma, X. Estimating the Least Principal Stress in a Granitic Rock Mass: Systematic Mini-Frac Tests and Elaborated Pressure Transient Analysis. *Rock Mech Rock Eng* 55, 1931–1954 (2022). <https://doi.org/10.1007/s00603-021-02743-1>

Doetsch, J., Krietsch, H., Schmelzbach, C., Jalali, M., Gischig, V., Villiger, L., Amann, F., & Maurer, H. (2020). Characterizing a decametre-scale granitic reservoir using ground-penetrating radar and seismic methods. *Solid Earth*, 11(4), 1441–1455. <https://doi.org/10.5194/se-11-1441-2020>

Horne, S. A. (2013). A statistical review of mudrock elastic anisotropy. *Geophysical Prospecting*, 61(4), 817–826. <https://doi.org/10.1111/1365-2478.12036>

Palmström, A., & Strömme, B. (1996). The Weighted Joint Density Method Leads to Improved Characterization of Jointing. *Conference on Recent Advances in Tunnelling Technology*.

Terzaghi, R. D. (1965). Sources of Error in Jopint Surveys. *Géotechnique*, 15, 287–304. <https://doi.org/https://doi.org/10.1680/geot.1965.15.3.287>

Thomsen, L. (1986). Weak elastic anisotropy. *Geophysics*, 51(10), 1954–1966. <https://doi.org/10.1190/1.1442051>